GKSS
FORSCHUNGSZENTRUM
in der HELMHOLTZ-GEMEINSCHAFT

Preprint 01-2009

Towards variational constitutive updates for non-associative plasticity models at finite strain: models based on a volumetric-deviatoric split

J. Mosler & O.T. Bruhns

This is a preprint of an article accepted by:

International Journal of Solids and Structures (2009)

GKSS Research Centre Geesthacht
Materials Mechanics

Towards variational constitutive updates for non-associative plasticity models at finite strain: models based on a volumetric-deviatoric split

J. Mosler

Materials Mechanics
Institute for Materials Research
GKSS Research Centre
D-21502 Geesthacht, Germany
E-Mail: joern.mosler@gkss.de

O.T. Bruhns

Institute of Mechanics
Ruhr University Bochum
Ruhr University Bochum
D-44780 Bochum, Germany
E-Mail: bruhns@tm.bi.rub.de

SUMMARY

In this paper, an enhanced *variational constitutive update* suitable for a class of non-associative plasticity theories at finite strain is proposed. In line with classical numerical formulations for plasticity models, such as the by now established return-mapping algorithm, *variational constitutive updates* represent a numerical method for computing the unknown state variables. However, in contrast to conventional algorithms, *variational constitutive updates* are fully variational, i.e., all unknown variables follow jointly from minimizing a certain potential. In addition to the physical and mathematical elegance of these variational schemes, they show several practical advantages as well. For instance, numerically efficient and robust optimization schemes can be directly employed for solving the resulting minimization problem. Since mathematically, plasticity is a non-smooth problem and often, it leads to highly singular systems of equations as known from single crystal plasticity, a robust implementation is of utmost importance. So far, *variational constitutive updates* have been developed for different classes of standard dissipative solids, i.e., solids characterized by associative evolution equations and flow rules. In the present paper, this framework is extended to a certain class of non-associative plasticity models at finite strain. All models falling into this class show a volumetric-deviatoric split of the Helmholtz energy and the yield function. Typical prototypes are Drucker-Prager or Mohr-Coulomb models playing an important role in soil mechanics. The efficiency and robustness of the resulting algorithmic formulation is demonstrated by means of selected numerical examples.

1 Introduction

Variational principles such as the minimum of the potential energy or Hamilton's principle have been playing an important role in classical mechanics for several centuries. These methods continue to be widely used in modern (i.e., computational) mechanics. More precisely, since almost every numerical scheme is based on variational principles, the importance of such approaches is continuously increasing. The probably best known development is given by the finite element method (of Bubnov-Galerkin-type).

In the present paper, focus is on a certain subset of variational methods, also known as *variational constitutive updates*. Conceptually in line with the pioneering work by von Mises to whom the postulate of maximum dissipation is usually credited (see [1]), variational constitutive updates allow to recast plasticity theories into equivalent minimization problems, cf. [2–7].

More specifically, every constitutive model falling into the range of so-called *standard dissipative solids* in the sense of Halphen & Nguyen [8] (see also [9]) can be implemented by applying the aforementioned concept. The advantages resulting from such a variational constitutive update are manifold. On the one hand, the existence of solutions can be analyzed by using the same tools originally designed for hyperelastic material models, cf. [5, 10, 11]. On the other hand, a minimum principle can be taken as a canonical basis for error estimation and thus, for adaptive finite element methods, cf. [3, 12–14].

Variational constitutive updates date back, at least, to the pioneering works by Comi and co-workers, cf. [6, 7]. By recourse to time discretization, these authors, derived a Hu-Washizu functional whose minimum corresponds to the solution of the discretized algebraic differential equations defining the constitutive model. In contrast to by now classical computational plasticity [15, 16], the underlying constitutive model was enforced in a weak sense. The ideas proposed by Comi and co-workers were further elaborated by Ortiz and co-workers, cf. [2, 3]. In line with the standard one-field description (the deformation mapping) usually applied in computational plasticity, Ortiz considered the constitutive model in a pointwise manner (at the integration points). By doing so, the minimization problem associated with variational constitutive updates can be decomposed into two subproblems. The first of those is purely local and its solution gives the updated state variables together with a reduced incremental potential. The second minimization problem depending on the aforementioned potential is global in nature and yields the unknown deformation mapping. Clearly, this structure coincides with standard computational plasticity, see [15, 16] and allows to separate the constitutive model from the governing equations. Evidently, this is very convenient from an implementational point of view.

Since the works by Comi and co-workers [6, 7] and the contributions by Ortiz and co-workers [2, 3], variational constitutive updates represent an active and ongoing research area, cf. [4, 5, 13, 17–21], and they are continuously further elaborated. For instance, the extensions necessary to include temperature effects were discussed in [22, 23]. A novel numerical implementation covering isotropic and kinematic hardening as well as isotropic and anisotropic elasticity and yield functions was advocated in [24].

Although the algorithmic framework proposed in [24] can be applied to a broad range of different constitutive models, it still relies on the assumptions associated with *standard dissipative solids* in the sense of Halphen & Nguyen [8]. More precisely, all material models belonging to the class of standard dissipative solids are defined by means of only two potentials being the Helmholtz energy and the yield function. Consequently, the plastic flow and hardening mechanisms are assumed to be governed by associative laws (normality rule). In other words and focusing on plasticity theory for now, the plastic potential and the hardening potential are identical to the yield function.

The present paper represents a first step towards generalizing variational constitutive updates to non-associative plasticity models at finite strain. For that purpose, three potentials are utilized: the Helmholtz energy, the yield function and a plastic potential. Roughly speaking, the idea is to minimize the integrated stress power subjected to the constraints imposed by the yield function. For a prototype model based on a volumetric-deviatoric split of all potentials, it is shown to that this constrained model can be recast into an equivalent unconstrained minimization problem. For that purpose, additional assumptions are necessary: the yield function and the plastic potential are represented by positively homogeneous functions of degree one and the plastic flow is either purely volumetric or purely deviatoric. While the first assumption is not very restrictive, the latter is indeed more drastic. However, it is noteworthy that both assumptions are fulfilled for many constitutive models frequently applied in soil mechanics. For instance, non-associative Drucker-Prager- or Mohr-Coulomb-type models with a deviatoric flow rule comply with the aforementioned restrictions.

The paper is organized as follows: In Section 2, a concise state-of-the-art review on variational constitutive updates is given. First, the fundamentals associated with finite strain plasticity theory based on a multiplicative decomposition of the deformation gradient are briefly presented for the sake of notation, cf. Subsection 2.1. Subsequently, standard dissipative solids, together with their defining variational framework, are discussed in Subsection 2.2. Section 2 is completed by an efficient numerical implementation for the aforementioned models (Subsection 2.3). The main contribution of the present paper dealing with a novel numerical implementation suitable for a class of non-associative plasticity theories is addressed in Section 3. Starting with the assumptions concerning the hyperelastic response (Subsection 3.1) and the plastic behavior (Subsection 3.2), a class of non-associative elastoplastic models is defined. Finally, the numerical implementation of this class is presented in Subsection 3.3. The efficiency and performance of the resulting constitutive update is demonstrated by means of selected numerical examples (Section 4).

2 Standard dissipative solids – Variational constitutive updates

This section is concerned with a concise review and some further elaborations associated with variational constitutive updates for standard dissipative solids, i.e., solids governed by normality rules.

2.1 Finite strain plasticity theory – Fundamentals

For the sake of concreteness, focus is on finite strain plasticity theory based on a multiplicative decomposition of the deformation gradient $\boldsymbol{F} := \mathrm{GRAD}\boldsymbol{\varphi}$ into an elastic part $\boldsymbol{F}^{\mathrm{e}}$ and a plastic part $\boldsymbol{F}^{\mathrm{p}}$ of the type

$$\boldsymbol{F} = \boldsymbol{F}^{\mathrm{e}} \cdot \boldsymbol{F}^{\mathrm{p}}, \qquad \text{with} \qquad \det \boldsymbol{F}^{\mathrm{e}} > 0, \ \det \boldsymbol{F}^{\mathrm{p}} > 0, \tag{1}$$

cf. [25]. Applying the split (1), the Helmholtz energy of the considered solid can be written as

$$\Psi = \Psi(\boldsymbol{F}^{\mathrm{e}}, \boldsymbol{\alpha}) \tag{2}$$

see [15, 16, 26, 27]. Here and henceforth, $\boldsymbol{\alpha} \in \mathbb{R}^n$ denotes a collection of some suitable strain-like internal variables corresponding to hardening or softening. In line with plasticity theory, the elastic response characterized by the elastic free energy $\bar{\Psi}^{\mathrm{e}}$ depends only on the elastic part of the deformation gradient $\boldsymbol{F}^{\mathrm{e}}$ and thus, the resulting Helmholtz energy decomposes additively, i.e.,

$$\Psi = \bar{\Psi}^{\mathrm{e}}(\boldsymbol{F}^{\mathrm{e}}) + \Psi^{\mathrm{p}}(\boldsymbol{\alpha}) \tag{3}$$

with Ψ^{p} representing the stored energy due to plastic work. Finally, by enforcing the principle of material frame indifference, Eq. (3) can be re-written as

$$\Psi = \Psi^{\mathrm{e}}(\boldsymbol{C}^{\mathrm{e}}) + \Psi^{\mathrm{p}}(\boldsymbol{\alpha}), \qquad \boldsymbol{C}^{\mathrm{e}} := \boldsymbol{F}^{\mathrm{e}T} \cdot \boldsymbol{F}^{\mathrm{e}}. \tag{4}$$

Further details are omitted. They may be found, e.g., in [28].

Adopting the framework of rational thermodynamics in the sense of Coleman & Noll [29–31], the evolution equations completing the constitutive model are derived by means of the

restrictions imposed by the second law of thermodynamics. For isothermal conditions, the dissipation inequality $\mathcal{D} \geq 0$ reads

$$\mathcal{D} = \left(\boldsymbol{F}^{\mathrm{p}} \cdot \boldsymbol{S} \cdot \boldsymbol{F}^{p^T} - 2 \, \frac{\partial \Psi}{\partial \boldsymbol{C}^{\mathrm{e}}} \right) : \frac{1}{2} \, \dot{\boldsymbol{C}}^{\mathrm{e}} + \boldsymbol{S} : \left(\boldsymbol{F}^{\mathrm{p}^T} \cdot \boldsymbol{C}^{\mathrm{e}} \cdot \dot{\boldsymbol{F}}^{\mathrm{p}} \right) + \boldsymbol{Q} \cdot \dot{\boldsymbol{\alpha}} \geq 0 \tag{5}$$

with $\boldsymbol{P}$ and $\boldsymbol{S} := \boldsymbol{F}^{-1} \cdot \boldsymbol{P}$ being the first and the second Piola-Kirchhoff stress tensor and $\boldsymbol{Q} := -\partial_{\boldsymbol{\alpha}} \Psi$ denoting the stress-like internal variable work conjugate to $\boldsymbol{\alpha}$. Ineq. (5), together with the by now standard procedure by Coleman & Noll, gives rise to

$$\boldsymbol{S} = 2 \, \frac{\partial \Psi}{\partial \boldsymbol{C}} = 2 \, \boldsymbol{F}^{\mathrm{p}^{-1}} \cdot \frac{\partial \Psi}{\partial \boldsymbol{C}^{\mathrm{e}}} \cdot \boldsymbol{F}^{\mathrm{p}^{-T}} \tag{6}$$

and the reduced dissipation inequality

$$\mathcal{D} = \boldsymbol{\Sigma} : \boldsymbol{L}^{\mathrm{p}} + \boldsymbol{Q} \cdot \dot{\boldsymbol{\alpha}} \geq 0. \tag{7}$$

Here, $\boldsymbol{\Sigma} = 2 \, \boldsymbol{C}^{\mathrm{e}} \cdot \partial_{\boldsymbol{C}^{\mathrm{e}}} \Psi$ are the Mandel stresses (cf. [32]) and $\boldsymbol{L}^{\mathrm{p}} = \dot{\boldsymbol{F}}^{\mathrm{p}} \cdot \boldsymbol{F}^{\mathrm{p}^{-1}}$ is the plastic velocity gradient. Evidently, both objects belong to the intermediate configuration induced by the multiplicative split (1). It is obvious that Ineq. (7) alone is not sufficient for deriving evolution equations for $\boldsymbol{L}^{\mathrm{p}}$ and $\dot{\boldsymbol{\alpha}}$, respectively. More precisely, loading conditions are needed.

For deciding whether purely elastic unloading or plastic loading occurs, a switch is required. For that purpose and following classical plasticity theory, an admissible stress space $\mathbb{E}_{\boldsymbol{\sigma}}$ is introduced, cf. [26]. Consistently with Ineq. (7), $\mathbb{E}_{\boldsymbol{\sigma}}$ is formulated in terms of Mandel stresses, i. e.,

$$\mathbb{E}_{\boldsymbol{\sigma}} = \left\{ (\boldsymbol{\Sigma}, \boldsymbol{Q}) \in \mathbb{R}^{9+n} \;\middle|\; \phi(\boldsymbol{\Sigma}, \boldsymbol{Q}) \leq 0 \right\}. \tag{8}$$

Here and henceforth, ϕ is the yield function. It has to be convex, sufficiently smooth and to comply with restrictions imposed by experimental observations. As well known, if $(\boldsymbol{\Sigma}, \boldsymbol{Q}) \in \mathrm{int}\mathbb{E}_{\boldsymbol{\sigma}}$, the solid deforms purely elastically. Only if $(\boldsymbol{\Sigma}, \boldsymbol{Q}) \in \partial\mathbb{E}_{\boldsymbol{\sigma}}$, a plastic response is possible.

Combining Eq. (8) and Ineq. (7), the evolution equations for $\boldsymbol{L}^{\mathrm{p}}$ and $\boldsymbol{\alpha}$ can be derived. They can be naturally obtained from the postulate of maximum dissipation, i.e.,

$$\max_{(\tilde{\boldsymbol{\Sigma}}, \tilde{\boldsymbol{Q}}) \in \mathbb{E}_{\boldsymbol{\sigma}}} \left[\tilde{\boldsymbol{\Sigma}} : \boldsymbol{L}^{\mathrm{p}} + \tilde{\boldsymbol{Q}} \cdot \dot{\boldsymbol{\alpha}} \right] \tag{9}$$

resulting in

$$\boldsymbol{L}^{\mathrm{p}} = \lambda \, \partial_{\boldsymbol{\Sigma}} \phi \qquad \dot{\boldsymbol{\alpha}} = \lambda \, \partial_{\boldsymbol{Q}} \phi, \tag{10}$$

together with the Karush-Kuhn-Tucker conditions

$$\lambda \geq 0 \qquad \phi \, \lambda \geq 0. \tag{11}$$

As a result, plastic deformations ($\boldsymbol{L}^{\mathrm{p}} \neq \boldsymbol{0}$) require $(\boldsymbol{\Sigma}, \boldsymbol{Q}) \in \partial\mathbb{E}_{\boldsymbol{\sigma}}$. The plastic multiplier λ is obtained from the consistency condition

$$\dot{\phi} = 0. \tag{12}$$

Evolution laws of the type (10) are characterized by the property that the rates of the internal variables (together with $\boldsymbol{L}^{\mathrm{p}}$) are normal to the yieldsurface ($\phi = 0$). Clearly, such laws are referred to as *associated flow rules* or *normality rules*. In the present section, only such evolution laws will be considered.

2.2 Standard dissipative solids

The fundamentals of standard dissipative solids are addressed in this subsection. It follows to a large extent [2, 5]. The ultimate goal of this subsection is to recast the constitutive framework summarized before into an equivalent minimization problem.

Roughly speaking, the potential to be minimized is the stress power

$$\mathcal{P}(\dot{\boldsymbol{\varphi}}, \dot{\boldsymbol{F}}^{\mathrm{p}}, \dot{\boldsymbol{\alpha}}, \boldsymbol{\Sigma}, \boldsymbol{Q}) = \boldsymbol{P} : \dot{\boldsymbol{F}} = \dot{\Psi}(\dot{\boldsymbol{\varphi}}, \dot{\boldsymbol{F}}^{\mathrm{p}}, \dot{\boldsymbol{\alpha}}) + \mathcal{D}(\dot{\boldsymbol{F}}^{\mathrm{p}}, \dot{\boldsymbol{\alpha}}, \boldsymbol{\Sigma}, \boldsymbol{Q}). \tag{13}$$

Note that Eq. (13) makes only sense from a physical point of view, if the stresses $\boldsymbol{\Sigma}$ and the internal variables $\boldsymbol{Q}$ defining the plastic flow $\boldsymbol{L}^{\mathrm{p}}$ and the strain-like variables $\boldsymbol{\alpha}$, respectively, are admissible. Following [2, 5], this constraint can be enforced by introducing the characteristic function of $\mathbb{E}_{\boldsymbol{\sigma}}$, i.e.,

$$J(\boldsymbol{\Sigma}, \boldsymbol{Q}) := \begin{cases} 0 & \forall (\boldsymbol{\Sigma}, \boldsymbol{Q}) \in \mathbb{E}_{\boldsymbol{\sigma}} \\ \infty & \text{otherwise} \end{cases} . \tag{14}$$

With J, the constrained problem associated with Eq. (13) reads now

$$\tilde{\mathcal{E}}(\dot{\boldsymbol{\varphi}}, \dot{\boldsymbol{F}}^{\mathrm{p}}, \dot{\boldsymbol{\alpha}}, \boldsymbol{\Sigma}, \boldsymbol{Q}) = \mathcal{P}(\dot{\boldsymbol{\varphi}}, \dot{\boldsymbol{F}}^{\mathrm{p}}, \dot{\boldsymbol{\alpha}}, \boldsymbol{\Sigma}, \boldsymbol{Q}) + J(\boldsymbol{\Sigma}, \boldsymbol{Q}). \tag{15}$$

The interesting properties of the functional (15) become apparent, if the stationarity conditions are computed. A straightforward calculation yields

$$\begin{aligned} \delta_{(\boldsymbol{\Sigma}, \boldsymbol{Q})} \tilde{\mathcal{E}} = \boldsymbol{0} \qquad &\Rightarrow \qquad (\boldsymbol{L}^{\mathrm{p}}, \dot{\boldsymbol{\alpha}}) \in \partial J \\ \delta_{(\dot{\boldsymbol{\alpha}})} \tilde{\mathcal{E}} = \boldsymbol{0} \qquad &\Rightarrow \qquad \boldsymbol{Q} = -\frac{\partial \Psi}{\partial \boldsymbol{\alpha}} \\ \delta_{(\dot{\boldsymbol{F}}^{\mathrm{p}})} \tilde{\mathcal{E}} = \boldsymbol{0} \qquad &\Rightarrow \qquad \boldsymbol{\Sigma} = \boldsymbol{F}^{\mathrm{e}^T} \cdot \frac{\partial \Psi}{\partial \boldsymbol{F}^{\mathrm{e}}} = 2\, \boldsymbol{C}^{\mathrm{e}} \cdot \frac{\partial \Psi}{\partial \boldsymbol{C}^{\mathrm{e}}}. \end{aligned} \tag{16}$$

Here, ∂J is the subdifferential of J, cf. [33]. According to Eqs. (16), the stationarity condition of $\tilde{\mathcal{E}}$ results in the flow rule, the constitutive relation for the internal stress-like variables and the constitutive relation for the Mandel stresses $\boldsymbol{\Sigma}$.

So far, a stationarity principle equivalent to associative plasticity theory at finite strain has been discussed. It can be shown that mathematically, this principle is represented by a saddle point problem (minimization with respect to ($\dot{\boldsymbol{\alpha}}$, $\dot{\boldsymbol{F}}^{\mathrm{p}}$), maximization with respect to ($\boldsymbol{\Sigma}$, $\boldsymbol{Q}$)). However, as advocated in [2, 5], it is possible to derive a reduced functional whose minimum yields the evolution equations. For that purpose the dual of J (the dissipation), i.e.,

$$J^*(\bar{\boldsymbol{L}}^{\mathrm{p}}, \dot{\bar{\boldsymbol{\alpha}}}) = \sup \left\{ \boldsymbol{\Sigma} : \bar{\boldsymbol{L}}^{\mathrm{p}} + \boldsymbol{Q} \cdot \dot{\bar{\boldsymbol{\alpha}}} \;\middle|\; (\boldsymbol{\Sigma}, \boldsymbol{Q}) \in \mathbb{E}_{\boldsymbol{\sigma}} \right\}, \tag{17}$$

defined by a Legendre transformation is required. Inserting the reduced dissipation Ineq. (7) into the stress power (13) and subsequently, into Eq. (15), together with the Legendre transformation (17), yields finally the reduced counterpart of Eq. (15)

$$\mathcal{E}(\dot{\boldsymbol{\varphi}}, \dot{\boldsymbol{F}}^{\mathrm{p}}, \dot{\boldsymbol{\alpha}}) = \dot{\Psi}(\dot{\boldsymbol{\varphi}}, \dot{\boldsymbol{F}}^{\mathrm{p}}, \dot{\boldsymbol{\alpha}}) + J^*(\boldsymbol{L}^{\mathrm{p}}, \dot{\boldsymbol{\alpha}}). \tag{18}$$

Hence, the only unknown variables are $\dot{\boldsymbol{\varphi}}$, $\dot{\boldsymbol{F}}^{\mathrm{p}}$ and $\dot{\boldsymbol{\alpha}}$. They follow jointly from the minimization principle

$$\overset{\circ}{\Psi}_{\mathrm{red}}(\dot{\boldsymbol{\varphi}}) := \inf_{\dot{\boldsymbol{F}}^{\mathrm{p}}, \dot{\boldsymbol{\alpha}}} \mathcal{E}(\dot{\boldsymbol{\varphi}}, \dot{\boldsymbol{F}}^{\mathrm{p}}, \dot{\boldsymbol{\alpha}}) \tag{19}$$

which, itself, gives rise to the introduction of the reduced functional $\overset{\circ}{\Psi}_{\mathrm{red}}$ depending only on the deformation mapping. Furthermore, by recalling that $\overset{\circ}{\Psi}_{\mathrm{red}}$ represents indeed the stress power and making use of Eq. (13), the first Piola Kirchhoff stress tensor results conveniently from

$$\boldsymbol{P} = \partial_{(\dot{\boldsymbol{F}})} \overset{\circ}{\Psi}_{\mathrm{red}}(\dot{\boldsymbol{\varphi}}). \tag{20}$$

As evident, this equation is identical to that of standard hyperelasticity with the sole exception that the potential $\overset{\circ}{\Psi}_{\rm red}$ is incrementally defined, i.e., it varies in time. For a more detailed derivation of the variational framework addressed in this subsection, the interested reader is referred to [2, 5].

2.3 Numerical implementation

The numerical implementation of the variational method discussed before, depends heavily on the Legendre transformation (17). Clearly, this transformation, in turn, is affected by the yield function. For the sake of concreteness, ϕ is assumed to be of the type

$$\phi = \Sigma^{\rm eq}(\boldsymbol{\Sigma} - \boldsymbol{Q}_{\rm k}) - Q_{\rm i}(\alpha_{\rm i}) - Q_0^{\rm eq} \tag{21}$$

with $\Sigma^{\rm eq}$, $\boldsymbol{Q}_{\rm k}$, $Q_{\rm i}$ and $Q_0^{\rm eq}$ denoting an equivalent stress, a backstress tensor, a stress-like internal variable associated with isotropic hardening and the initial yield strength, respectively. Furthermore, $\boldsymbol{\alpha}_{\rm k}$ and $\alpha_{\rm i}$ represent the strain-like variables conjugate to $\boldsymbol{Q}_{\rm k}$ and $Q_{\rm i}$. If $\boldsymbol{Q}_{\rm k}$ and $Q_{\rm i}$ are stress-like, $\Sigma^{\rm eq}$ should be a linear mapping. More precisely, $\Sigma^{\rm eq}$ is chosen to be a positively homogeneous function of degree one. This restriction is fulfilled for many yield functions such as Rankine, von Mises, Hill, Drucker-Prager, Tresca, Mohr-Coulomb or crystal plasticity. Positive homogeneity implies

$$\Sigma^{\rm eq} = \partial_{\boldsymbol{\Sigma}}\Sigma^{\rm eq} : \boldsymbol{\Sigma} = \partial_{\boldsymbol{\Sigma}}\phi : \boldsymbol{\Sigma} \tag{22}$$

and consequently,

$$\begin{aligned} {\rm d}\Sigma^{\rm eq} &= \partial_{\boldsymbol{\Sigma}}\Sigma^{\rm eq} : {\rm d}\boldsymbol{\Sigma} = \partial_{\boldsymbol{\Sigma}}\phi : {\rm d}\boldsymbol{\Sigma} \\ &= \partial_{\boldsymbol{\Sigma}}[\partial_{\boldsymbol{\Sigma}}\phi : \boldsymbol{\Sigma}] : {\rm d}\boldsymbol{\Sigma} = \partial_{\boldsymbol{\Sigma}}\phi : {\rm d}\boldsymbol{\Sigma} + [\boldsymbol{\Sigma} : \partial^2_{\boldsymbol{\Sigma}\boldsymbol{\Sigma}}\phi] : {\rm d}\boldsymbol{\Sigma} \\ &\Rightarrow \quad \boxed{\boldsymbol{\Sigma} : \partial^2_{\boldsymbol{\Sigma}\boldsymbol{\Sigma}}\phi = \boldsymbol{0}}. \end{aligned} \tag{23}$$

This conditions will be used for proving consistency of the algorithm. By postulating associative evolution equations, they are obtained from Eq. (21) as

$$\boldsymbol{L}^{\rm p} = \lambda\, \partial_{\boldsymbol{\Sigma}}\phi, \qquad \dot{\boldsymbol{\alpha}}_{\rm k} = \lambda\, \partial_{\boldsymbol{Q}}\phi = -\lambda\, \partial_{\boldsymbol{\Sigma}}\phi, \qquad \dot{\alpha}_{\rm i} = -\lambda \tag{24}$$

Inserting Eqs. (24) into the dissipation (7), the second law of thermodynamics yields

$$\mathcal{D} \overset{\phi=0}{=} \lambda\, Q_0^{\rm eq} \geq 0. \tag{25}$$

and thus, the (reduced) stress power reads

$$\mathcal{E} = \dot{\Psi} + \lambda\, Q_0^{\rm eq}. \tag{26}$$

Clearly, Eq. (26) is only physically meaningful for admissible evolution equations, cf. Eq. (10). Furthermore, note that the necessary yield condition $\phi = 0$ is already naturally included (see Eq. (25)).

Conceptionally, variational constitutive updates are simply an approximation of the minimization problem (19). A first step towards this approximation is obtained by applying a time integration to Eq. (19), i.e.,

$$(\boldsymbol{F}^{\rm p}, \boldsymbol{\alpha}_{\rm k}, \alpha_{\rm i}) = \arg\inf I^{\rm ana}_{\rm inc}, \tag{27}$$

with

$$I^{\rm ana}_{\rm inc} = \int_{t_n}^{t_{n+1}} \mathcal{E}\ {\rm d}t = \Psi_{n+1} - \Psi_n + Q_0^{\rm eq}\, \Delta\lambda \tag{28}$$

Here, the notations $\Delta\lambda := \int_{t_n}^{t_{n+1}} \lambda \; \mathrm{d}t$ and $(\bullet)_n := (\bullet)(t_n)$ have been introduced. The superscript $(\bullet)^{\mathrm{ana}}$ is used to highlight that $I_{\mathrm{inc}}^{\mathrm{ana}}$ results from an analytical integration. Note that the unknowns $(\boldsymbol{F}^{\mathrm{p}}, \boldsymbol{\alpha}_{\mathrm{k}}, \alpha_{\mathrm{i}})$ are functions (in time). In line with [2, 5], a discrete approximation of Eq. (28) is derived by using a time discretization of the type

$$\begin{array}{lcl} \boldsymbol{F}^{\mathrm{p}}_{n+1} & = & \exp\left[\Delta\lambda \;\; \partial_{\boldsymbol{\Sigma}}\phi|_{n+1}\right] \cdot \boldsymbol{F}^{\mathrm{p}}_{n} \\ \alpha_{\mathrm{i}}|_{n+1} & = & \alpha_{\mathrm{i}}|_{n} - \Delta\lambda \\ \boldsymbol{\alpha}_{\mathrm{k}}|_{n+1} & = & \boldsymbol{\alpha}_{\mathrm{k}}|_{n} - \Delta\lambda \;\; \partial_{\boldsymbol{\Sigma}}\phi|_{n+1} \, . \end{array} \tag{29}$$

Clearly, other consistent time integration can be employed as well, cf. [24]. With Eqs. (29), the discrete (approximated) counterpart of minimization problem (27) can be written as

$$(\boldsymbol{F}^{\mathrm{p}}_{n+1}, \boldsymbol{\alpha}_{\mathrm{k}}|_{n+1}, \alpha_{\mathrm{i}}|_{n+1}) = \arg\inf I_{\mathrm{inc}}, \tag{30}$$

with

$$I_{\mathrm{inc}} = \Psi_{n+1}(\boldsymbol{F}^{\mathrm{p}}_{n+1}, \boldsymbol{\alpha}_{\mathrm{k}}|_{n+1}, \alpha_{\mathrm{i}}|_{n+1}) - \Psi_n + Q_0^{\mathrm{eq}} \; \Delta\lambda \approx I_{\mathrm{inc}}^{\mathrm{ana}}. \tag{31}$$

So far, variational constitutive updates are relatively simple and hence, the respective implementation seems to be straightforward. Unfortunately, this is not the case. The reasons for that are manifold. For instance, a direct minimization of Ψ_{inc} with respect to $\boldsymbol{F}^{\mathrm{p}}_{n+1}$ is not admissible, since $\boldsymbol{F}^{\mathrm{p}}$ has to comply with physical constraints resulting from the flow rule (and of course, $\det \boldsymbol{F}^{\mathrm{p}} > 0$).

Recently, a convenient parameterization of the evolution equations (29) was given in [24]. By introducing pseudo stresses $\tilde{\boldsymbol{\Sigma}}$ which are not identical to their physical counterparts, i.e., $\tilde{\boldsymbol{\Sigma}} \neq \boldsymbol{\Sigma}$, Eqs. (29) are re-formulated as

$$\begin{array}{lcl} \boldsymbol{F}^{\mathrm{p}}_{n+1}(\tilde{\boldsymbol{\Sigma}}, a) & = & \exp\left[a^2 \;\; \partial_{\boldsymbol{\Sigma}}\phi|_{\tilde{\boldsymbol{\Sigma}}}\right] \cdot \boldsymbol{F}^{\mathrm{p}}_{n} \\ \alpha_{\mathrm{i}}|_{n+1}\,(a) & = & \alpha_{\mathrm{i}}|_{n} - a^2 \\ \boldsymbol{\alpha}_{\mathrm{k}}|_{n+1}\,(\tilde{\boldsymbol{\Sigma}}, a) & = & \boldsymbol{\alpha}_{\mathrm{k}}|_{n} - a^2 \; \partial_{\boldsymbol{\Sigma}}\phi|_{\tilde{\boldsymbol{\Sigma}}} \, . \end{array} \tag{32}$$

Consequently, $\tilde{\boldsymbol{\Sigma}}$ can be interpreted as an unknown variable defining the flow direction, i.e., $\partial_{\boldsymbol{\Sigma}}\phi|_{\boldsymbol{\Sigma}} = \partial_{\boldsymbol{\Sigma}}\phi|_{\tilde{\boldsymbol{\Sigma}}}$, and $a^2 := \lambda \geq 0$. Making use of Eq. (32) allows to re-write Eq. (30) as

$$\boldsymbol{X} = \arg\inf_{\boldsymbol{X}} I_{\mathrm{inc}}(\boldsymbol{X}), \quad \text{with} \quad I_{\mathrm{inc}} = \Psi_{n+1}(\boldsymbol{X}) - \Psi_n + Q_0^{\mathrm{eq}} \; \Delta\lambda \tag{33}$$

with the unknowns being

$$\boldsymbol{X} = [\tilde{\boldsymbol{\Sigma}}, a] \quad \Rightarrow \quad \dim[\boldsymbol{X}] = 10. \tag{34}$$

It is noteworthy that the unconstrained optimization problem (33) includes naturally the necessary yielding condition $\phi = 0$, and admissible evolution equations are canonically included as well. Further details are omitted. They may be found in [24].

The unconstrained minimization problem (33) can be solved in a standard manner, e.g., by employing gradient-type schemes, cf. [34]. The first derivatives of I_{inc} are summarized below,

$$\frac{\partial I_{\mathrm{inc}}}{\partial \Delta\lambda} = \frac{\partial \Psi^{\mathrm{e}}}{\partial \Delta\lambda} + \frac{\partial \Psi^{\mathrm{p}}}{\partial \Delta\lambda} + Q_0^{\mathrm{eq}} \tag{35}$$

$$\frac{\partial I_{\mathrm{inc}}}{\partial \tilde{\boldsymbol{\Sigma}}} = \frac{\partial \Psi^{\mathrm{e}}}{\partial \tilde{\boldsymbol{\Sigma}}} + \frac{\partial \Psi^{\mathrm{p}}}{\partial \tilde{\boldsymbol{\Sigma}}}, \tag{36}$$

with

$$\frac{\partial \Psi^{\mathrm{e}}}{\partial \Delta\lambda} = -\left[(\boldsymbol{F}^{\mathrm{e}}_{\mathrm{trial}})^T \cdot \frac{\partial \Psi^{\mathrm{e}}}{\partial \boldsymbol{F}^{\mathrm{e}}}\right] : D\exp\left[-\Delta\lambda\, \partial_{\boldsymbol{\Sigma}}\phi|_{\tilde{\boldsymbol{\Sigma}}}\right] : \partial_{\boldsymbol{\Sigma}}\phi|_{\tilde{\boldsymbol{\Sigma}}}\,, \tag{37}$$

$$\frac{\partial \Psi^{\mathrm{e}}}{\partial \tilde{\boldsymbol{\Sigma}}} = -\left[(\boldsymbol{F}^{\mathrm{e}}_{\mathrm{trial}})^T \cdot \frac{\partial \Psi^{\mathrm{e}}}{\partial \boldsymbol{F}^{\mathrm{e}}}\right] : D\exp\left[-\Delta\lambda\, \partial_{\boldsymbol{\Sigma}}\phi|_{\tilde{\boldsymbol{\Sigma}}}\right] : \partial^2_{\boldsymbol{\Sigma}}\phi\big|_{\tilde{\boldsymbol{\Sigma}}}\; \Delta\lambda, \tag{38}$$

$$\frac{\partial \Psi^{\mathrm{p}}}{\partial \Delta\lambda} = Q_{\mathrm{i}} + \boldsymbol{Q}_{\mathrm{k}} : \partial_{\boldsymbol{\Sigma}}\phi|_{\tilde{\boldsymbol{\Sigma}}}\,, \tag{39}$$

$$\frac{\partial \Psi^{\mathrm{p}}}{\partial \tilde{\boldsymbol{\Sigma}}} = \frac{\partial \Psi^{\mathrm{p}}}{\partial \boldsymbol{\alpha}_{\mathrm{k}}} : \frac{\partial \boldsymbol{\alpha}_{\mathrm{k}}}{\partial \tilde{\boldsymbol{\Sigma}}} = \Delta\lambda\, \boldsymbol{Q}_{\mathrm{k}} : \partial^2_{\boldsymbol{\Sigma}}\phi\big|_{\tilde{\boldsymbol{\Sigma}}}\,. \tag{40}$$

with $\boldsymbol{F}^{\mathrm{e}}_{\mathrm{trial}}$ being the trial elastic deformation gradient, i.e.,

$$\boldsymbol{F}^{\mathrm{e}}_{\mathrm{trial}} := \boldsymbol{F}_{n+1} \cdot (\boldsymbol{F}^{\mathrm{p}}_{n})^{-1}. \tag{41}$$

In Eqs. (37) and (38), the derivative of the exponential mapping

$$D\exp[\boldsymbol{A}] := \frac{\partial \exp[\boldsymbol{A}]}{\partial \boldsymbol{A}} \tag{42}$$

can be computed in a standard fashion, e.g. [35, 36]. For the sake of brevity, the second derivatives necessary for a Newton-type iteration are omitted. However, they can be computed in a straightforward manner.

By analyzing the stationarity condition of I_{inc}, consistency of the algorithm can be checked. For instance, taking the variation of I_{inc} with respect to $\Delta\lambda$ and enforcing stationarity results in

$$\left.\frac{\partial I_{\mathrm{inc}}}{\partial \Delta\lambda}\right|_{\Delta t\to 0} = -\boldsymbol{\Sigma} : \partial_{\boldsymbol{\Sigma}}\phi + Q_i + \boldsymbol{Q}_{\mathrm{k}} : \partial_{\boldsymbol{\Sigma}}\phi + Q^{\mathrm{eq}}_{\mathrm{i}} = -\phi = 0, \tag{43}$$

i.e., the necessary condition for yielding. Furthermore, with $\boldsymbol{\Xi} := \boldsymbol{\Sigma} - \boldsymbol{Q}_{\mathrm{k}}$, the stationarity condition associated with the pseudo stresses $\tilde{\boldsymbol{\Sigma}}$ reads

$$\frac{\partial I_{\mathrm{inc}}}{\partial \tilde{\boldsymbol{\Sigma}}} = \boldsymbol{0} \quad \overset{\Delta\lambda\neq 0}{\Rightarrow} \quad (\boldsymbol{\Sigma} - \boldsymbol{Q}_{\mathrm{k}}) : \partial^2_{\boldsymbol{\Sigma}}\phi = \boldsymbol{\Xi} : \partial^2_{\boldsymbol{\Xi}}\phi = \boldsymbol{0}. \tag{44}$$

Hence, Eq. (23) is fulfilled and consequently, the plastic flow direction is compatible with the stresses and hence, it is admissible.

It bears emphasis that in line with conventional plasticity theory, the optimization problem $\inf I_{\mathrm{inc}}$ is non-smooth (with respect to $\Delta\lambda$). To sidestep this problem, predictor-corrector methods are usually applied, cf. Eq. (41). Following the return-mapping algorithm, a trial step characterized by a purely elastic response is assumed first ($\Delta\lambda = 0$, $\boldsymbol{F}^{\mathrm{p}}_{n+1} = \boldsymbol{F}^{\mathrm{p}}_{n}$, $\boldsymbol{Q}_{\mathrm{k}}|_{n+1} = \boldsymbol{Q}_{\mathrm{k}}|_{n}$ and $Q_{\mathrm{i}}|_{n+1} = Q_{\mathrm{i}}|_{n}$). Clearly, if this state is physically admissible, the functional I_{inc} has to show a minimum at $\Delta\lambda = 0$. With Eqs. (35)–(40) (cf. Eq. (43)), the respective condition yields

$$\left.\frac{\partial I_{\mathrm{inc}}}{\partial \Delta\lambda}\right|_{\Delta\lambda=0} = -\phi_{\mathrm{trial}} > 0 \quad \Longleftrightarrow \quad \phi_{\mathrm{trial}} \leq 0. \tag{45}$$

with $\phi_{\mathrm{trial}} := \phi(\boldsymbol{F}_{n+1}, \boldsymbol{F}^{\mathrm{p}}_{n}, Q_{\mathrm{i}}|_{n}, \boldsymbol{Q}_{\mathrm{k}}|_{n})$. Remarkably, this inequality agrees with that of the classical return-mapping algorithm. It is noteworthy, that the remaining components of the gradient of I_{inc} vanish trivially, i.e.,

$$\left.\frac{\partial I_{\mathrm{inc}}}{\partial \tilde{\boldsymbol{\Sigma}}}\right|_{\Delta\lambda=0} = \boldsymbol{0}. \tag{46}$$

Further details about the numerical implementation are omitted. They can be found in [24]. In the cited paper, a tuned algorithm for fully isotropic models is given as well.

3 A class of non-associative elastoplastic models based on a volumetric-deviatoric split: Plasticity theory at finite strains

Based on the variational constitutive update for standard dissipative solids as discussed in the previous section, the extensions necessary for non-associative plasticity theory are elaborated here. In contrast to the constitutive framework considered before, some more restrictive assumptions have to be introduced. More precisely, focus is on a class of non-associative plasticity models showing a volumetric-deviatoric uncoupled response.

3.1 Elasticity

Focusing on the elastic response for now, the first crucial assumption is the decomposition of the elastic free energy into a deviatoric and a volumetric part, cf. [37]. More specifically,

$$\Psi^{\mathrm{e}} = \Psi^{\mathrm{e}}_{\mathrm{dev}} + \Psi^{\mathrm{e}}_{\mathrm{vol}}, \quad \text{with} \quad \Psi^{\mathrm{e}}_{\mathrm{dev}} = \Psi^{\mathrm{e}}_{\mathrm{dev}}(\boldsymbol{C}^{\mathrm{e}}_{\mathrm{dev}}), \quad \Psi^{\mathrm{e}}_{\mathrm{vol}} = \Psi^{\mathrm{e}}_{\mathrm{vol}}(J^{\mathrm{e}}). \tag{47}$$

Here, the following notations have been introduced:

$$J^{\mathrm{e}} := \det \boldsymbol{F}^{\mathrm{e}}, \quad \boldsymbol{F}^{\mathrm{e}}_{\mathrm{dev}} := (J^{\mathrm{e}})^{-1/3}\, \boldsymbol{F}^{\mathrm{e}}, \quad \boldsymbol{C}^{\mathrm{e}}_{\mathrm{dev}} := (\boldsymbol{F}^{\mathrm{e}}_{\mathrm{dev}})^{T} \cdot \boldsymbol{F}^{\mathrm{e}}_{\mathrm{dev}} = (J^{\mathrm{e}})^{-2/3}\, \boldsymbol{C}^{\mathrm{e}}. \tag{48}$$

Eq. (47) yields the second Piola-Kirchhoff stresses (belonging to the intermediate configuration)

$$\boldsymbol{S}^{\mathrm{e}} := 2\, \partial_{\boldsymbol{C}^{\mathrm{e}}} \Psi^{\mathrm{e}} = J^{\mathrm{e}}\, \partial_{J^{\mathrm{e}}}[\Psi^{\mathrm{e}}_{\mathrm{vol}}]\, \boldsymbol{C}^{\mathrm{e}-1} + 2\, \partial_{\boldsymbol{C}^{\mathrm{e}}_{\mathrm{dev}}}[\Psi^{\mathrm{e}}_{\mathrm{dev}}] : \mathbb{P}_{\mathrm{dev}} \tag{49}$$

where

$$\mathbb{P}_{\mathrm{dev}} := \partial_{\boldsymbol{C}^{\mathrm{e}}} \boldsymbol{C}^{\mathrm{e}}_{\mathrm{dev}} = (J^{\mathrm{e}})^{-2/3} \left[\mathbb{I}^{\mathrm{sym}} - \frac{1}{3}\, \boldsymbol{C}^{\mathrm{e}} \otimes \boldsymbol{C}^{\mathrm{e}-1} \right] \tag{50}$$

is a projection tensor. Finally, the Mandel stress can be computed by using Eq. (47). They result in

$$\begin{aligned} \boldsymbol{\Sigma} := \boldsymbol{C}^{\mathrm{e}} \cdot \boldsymbol{S}^{\mathrm{e}} = \quad & J^{\mathrm{e}}\, \partial_{J^{\mathrm{e}}}[\Psi^{\mathrm{e}}_{\mathrm{vol}}]\, \mathbf{1} \\ + \quad & 2\, (J^{\mathrm{e}})^{-2/3} \left[\boldsymbol{C}^{\mathrm{e}} \cdot \partial_{\boldsymbol{C}^{\mathrm{e}}_{\mathrm{dev}}}[\Psi^{\mathrm{e}}_{\mathrm{dev}}] - \frac{1}{3} \left(\partial_{\boldsymbol{C}^{\mathrm{e}}_{\mathrm{dev}}}[\Psi^{\mathrm{e}}_{\mathrm{dev}}] : \boldsymbol{C}^{\mathrm{e}} \right)\, \mathbf{1} \right]. \end{aligned} \tag{51}$$

In this section, only yield functions and plastic potentials based on a similar split as that in Eq. (47) will be considered. For this reason, the volumetric as well as the deviatoric part of the stresses are required. With Eq. (47), they are obtained as

$$\mathrm{tr}[\boldsymbol{\Sigma}] = 3\, J^{\mathrm{e}}\, \partial_{J^{\mathrm{e}}}[\Psi^{\mathrm{e}}_{\mathrm{vol}}] \tag{52}$$

and

$$\mathrm{dev}\boldsymbol{\Sigma} := \boldsymbol{\Sigma} - \frac{1}{3}\, \mathrm{tr}[\boldsymbol{\Sigma}]\, \mathbf{1} = 2\, (J^{\mathrm{e}})^{-2/3} \left[\boldsymbol{C}^{\mathrm{e}} \cdot \partial_{\boldsymbol{C}^{\mathrm{e}}_{\mathrm{dev}}}[\Psi^{\mathrm{e}}_{\mathrm{dev}}] - \frac{1}{3} \left(\partial_{\boldsymbol{C}^{\mathrm{e}}_{\mathrm{dev}}}[\Psi^{\mathrm{e}}_{\mathrm{dev}}] : \boldsymbol{C}^{\mathrm{e}} \right)\, \mathbf{1} \right]. \tag{53}$$

3.2 Plasticity

Analogously to the elastic response, the considered class of yield functions is also characterized by a volumetric-deviatoric split, i.e.,

$$\phi = \Sigma^{\mathrm{eq}}_{\mathrm{vol}} + \Sigma^{\mathrm{eq}}_{\mathrm{dev}} - Q_{\mathrm{i}} - Q^{\mathrm{eq}}_{0} \tag{54}$$

with

$$\Sigma^{\rm eq}_{\rm vol} = \Sigma^{\rm eq}_{\rm vol}({\rm tr}[\boldsymbol{\Xi}]), \qquad \Sigma^{\rm eq}_{\rm dev} = \Sigma^{\rm eq}_{\rm dev}({\rm dev}[\boldsymbol{\Xi}]), \quad \text{and} \quad \boldsymbol{\Xi} := \boldsymbol{\Sigma} - \boldsymbol{Q}_{\rm k}. \tag{55}$$

Following Section 2, ϕ and consequently, $\Sigma^{\rm eq}_{\rm vol}$ and $\Sigma^{\rm eq}_{\rm dev}$ are assumed to be positively homogeneous functions of degree one, see Eq. (22). It is noteworthy that the yield function (54) covers a broad range of different plasticity models. For instance, by setting

$$\Sigma^{\rm eq}_{\rm vol} = \kappa\ {\rm tr}[\boldsymbol{\Xi}], \qquad \Sigma^{\rm eq}_{\rm dev} = ||{\rm dev}[\boldsymbol{\Xi}]||, \tag{56}$$

the Drucker-Prager model is obtained. Mohr-Coulomb's yield function is given by

$$\Sigma^{\rm eq}_{\rm vol} = \kappa\ {\rm tr}[\boldsymbol{\Xi}], \qquad \Sigma^{\rm eq}_{\rm dev} = \frac{1}{2}[\max \Sigma_i - \min \Sigma_i]. \tag{57}$$

Here, $\max \Sigma_i$ and $\min \Sigma_i$ are the largest and smallest eigenvalue of $\boldsymbol{\Sigma}$. It bears emphasis that $\Sigma^{\rm eq}_{\rm dev}$ according to Eq. (57) is indeed a positively homogeneous function of degree one. Finally, an anisotropic Drucker-Prager prototype is defined by using a Hill-type equivalent stress for the deviatoric part, i.e.,

$$\Sigma^{\rm eq}_{\rm vol} = \kappa\ {\rm tr}[\boldsymbol{\Xi}], \qquad \Sigma^{\rm eq}_{\rm dev} = \sqrt{{\rm dev}[\boldsymbol{\Xi}] : \mathbb{D} : {\rm dev}[\boldsymbol{\Xi}]}, \tag{58}$$

with $\mathbb{D}$ representing a fourth-order weighting tensor, cf. [24].

In contrast to the yield function (54), the plastic potential g defining the flow rule and the evolution equations is assumed to be purely deviatoric, i.e.,

$$g = \Sigma^{\rm eq}_{\rm dev} - Q_i - Q^{\rm eq}_0. \tag{59}$$

Consequently,

$$\boldsymbol{L}^{\rm p} = \lambda\ \partial_{\boldsymbol{\Sigma}} \Sigma^{\rm eq}_{\rm dev}, \quad \dot{\boldsymbol{\alpha}}_{\rm k} = -\lambda \partial_{\boldsymbol{\Sigma}} \Sigma^{\rm eq}_{\rm dev}, \quad \dot{\alpha}_{\rm i} = -\lambda. \tag{60}$$

Clearly, this represents a limiting case being important, for instance, in soil mechanics. Bearing in mind that $\Sigma^{\rm eq}_{\rm dev}$ is positively homogeneous of degree one, the dissipation is calculated as

$$\mathcal{D} = (\partial_{\boldsymbol{\Sigma}} g : \boldsymbol{\Sigma} - \partial_{\boldsymbol{\Sigma}} g : \boldsymbol{Q}_{\rm k} - Q_{\rm i})\ \lambda = (\Sigma^{\rm eq}_{\rm dev} - Q_i)\ \lambda \overset{\phi=0}{=} (Q^{\rm eq}_0 - \Sigma^{\rm eq}_{\rm vol})\ \lambda. \tag{61}$$

3.3 Numerical implementation

In this subsection, the algorithmic formulation associated with the constitutive model based on the volumetric-deviatoric split as introduced before, is presented. That is, focus is on plasticity theories fulfilling the restrictions (47), (54) and (59). It has already been mentioned, that this class covers a broad range of different important prototypes such as non-associative Drucker-Prager or Mohr-Coulomb plasticity.

3.3.1 Fundamentals of the algorithm

Analogously to Section 2, the evolution laws are approximated by a time integration and they are parameterized by the pseudo stresses $\tilde{\boldsymbol{\Sigma}}$ and the parameter $a = \sqrt{\Delta\lambda}$, i.e.,

$$\begin{array}{lcl} \boldsymbol{F}^{\rm p}_{n+1} & = & \exp\left[a^2\ \partial_{\boldsymbol{\Sigma}} g|_{\tilde{\boldsymbol{\Sigma}}}\right] \cdot \boldsymbol{F}^{\rm p}_n \\ \alpha_{\rm i}|_{n+1} & = & \alpha_{\rm i}|_n - a^2 \\ \boldsymbol{\alpha}_{\rm k}|_{n+1} & = & \boldsymbol{\alpha}_{\rm k}|_n - a^2\ \partial_{\boldsymbol{\Sigma}} g|_{\tilde{\boldsymbol{\Sigma}}}\,. \end{array} \tag{62}$$

Clearly, since the plastic flow is traceless (${\rm tr}[\partial_{\boldsymbol{\Sigma}} g] = \boldsymbol{0}$),

$$\det \boldsymbol{F}^{\rm p}_{n+1} = 1 \quad \Rightarrow \det \boldsymbol{F}^{\rm e}_{n+1} =: J^{\rm e} = J = \det \boldsymbol{F}. \tag{63}$$

Furthermore, the strain-like internal variable $\boldsymbol{\alpha}_{\mathrm{k}}$ is also purely deviatoric (if $\boldsymbol{\alpha}_{\mathrm{k}}(t=0)=\mathbf{0}$) and thus, it is physically reasonable to postulate

$$\mathrm{tr}[\boldsymbol{Q}_{\mathrm{k}}] = 0. \tag{64}$$

As a result, by using $\mathrm{tr}[\boldsymbol{\Sigma}]$ according to Eq. (52), together with Eq. (63),

$$\Sigma^{\mathrm{eq}}_{\mathrm{vol}}(\mathrm{tr}[\boldsymbol{\Sigma}-\boldsymbol{Q}_{\mathrm{k}}]) = \Sigma^{\mathrm{eq}}_{\mathrm{vol}}(\mathrm{tr}[\boldsymbol{\Sigma}]) = \Sigma^{\mathrm{eq}}_{\mathrm{vol}}(J^e) = \Sigma^{\mathrm{eq}}_{\mathrm{vol}}(J). \tag{65}$$

Hence, a backward-Euler integration of the dissipation (61)yields

$$\int_{t_n}^{t_{n+1}} \mathcal{D}\ \mathrm{d}t \approx \left(Q_0^{\mathrm{eq}} - \Sigma^{\mathrm{eq}}_{\mathrm{vol}}\big|_{n+1}\right)\ \Delta\lambda \tag{66}$$

and consequently, the integrated stress power is approximated as

$$I_{\mathrm{inc}}(\boldsymbol{X}) = \Psi_{n+1}(\boldsymbol{X}) - \Psi_n + \left(Q_0^{\mathrm{eq}} - \Sigma^{\mathrm{eq}}_{\mathrm{vol}}\big|_{n+1}\right)\ \Delta\lambda, \quad \boldsymbol{X} = [\tilde{\boldsymbol{\Sigma}}, a], \tag{67}$$

cf. Eq. (31). In line with the previous subsection, the potential $I_{\mathrm{inc}}(\boldsymbol{X})$ can be minimized in case of plastic loading by gradient-type optimization schemes. The first derivatives are summarized below:

$$\begin{aligned}\frac{\partial I_{\mathrm{inc}}}{\partial \Delta\lambda} = &- \left[(\boldsymbol{F}^{\mathrm{e}}_{\mathrm{trial}})^T \cdot \frac{\partial \Psi^{\mathrm{e}}}{\partial \boldsymbol{F}^{\mathrm{e}}}\right] : D\exp\left[-\Delta\lambda\ \partial_{\boldsymbol{\Sigma}} g|_{\tilde{\boldsymbol{\Sigma}}}\right] : \partial_{\boldsymbol{\Sigma}} g|_{\tilde{\boldsymbol{\Sigma}}} \\ &+ Q_{\mathrm{i}} + \boldsymbol{Q}_{\mathrm{k}} : \partial_{\boldsymbol{\Sigma}} g|_{\tilde{\boldsymbol{\Sigma}}} + Q_0^{\mathrm{eq}} - \Sigma^{\mathrm{eq}}_{\mathrm{vol}}\big|_{n+1}\end{aligned} \tag{68}$$

$$\begin{aligned}\frac{\partial I_{\mathrm{inc}}}{\partial \tilde{\boldsymbol{\Sigma}}} = &- \left[(\boldsymbol{F}^{\mathrm{e}}_{\mathrm{trial}})^T \cdot \frac{\partial \Psi^{\mathrm{e}}}{\partial \boldsymbol{F}^{\mathrm{e}}}\right] : D\exp\left[-\Delta\lambda\ \partial_{\boldsymbol{\Sigma}} g|_{\tilde{\boldsymbol{\Sigma}}}\right] : \partial^2_{\boldsymbol{\Sigma}} g\big|_{\tilde{\boldsymbol{\Sigma}}}\ \Delta\lambda \\ &+ \Delta\lambda\ \boldsymbol{Q}_{\mathrm{k}} : \partial^2_{\boldsymbol{\Sigma}} g\big|_{\tilde{\boldsymbol{\Sigma}}}.\end{aligned} \tag{69}$$

The second derivatives of $I_{\mathrm{inc}}(\boldsymbol{X})$ can be computed in a similar fashion. According to Eq. (67), only the Helmholtz energy depends on the pseudo stresses and thus, $\partial I_{\mathrm{inc}}/\partial\tilde{\boldsymbol{\Sigma}} = \partial\Psi/\partial\tilde{\boldsymbol{\Sigma}}$. Consequently, the gradient of I_{inc} with respect to $\tilde{\boldsymbol{\Sigma}}$ is identical to that of the associative model (compare Eq. (69) to Eq. (36)) with the sole exception that the yield function ϕ is replaced by the plastic potential g.

3.3.2 Consistency of the algorithm

Although the algorithm has been completely defined, it is not clear yet, if the method is consistent. Thus, a consistency analysis is given in this paragraph. In line with Section 2.3, the stationarity condition of I_{inc} with respect to the plastic multiplier $\Delta\lambda$ is considered first. Employing Eq. (68) and focusing on the limiting case $\Delta\lambda \to 0$, stationarity of I_{inc} requires

$$\left.\frac{\partial I_{\mathrm{inc}}}{\partial \Delta\lambda}\right|_{\Delta t\to 0} = -\underbrace{(\boldsymbol{\Sigma}-\boldsymbol{Q}_{\mathrm{k}}) : \partial_{\boldsymbol{\Sigma}} g}_{=\Sigma^{\mathrm{eq}}_{\mathrm{dev}}} + Q_{\mathrm{i}} + Q_0^{\mathrm{eq}} - \Sigma^{\mathrm{eq}}_{\mathrm{vol}} = -\phi = 0 \tag{70}$$

As a result, the yield condition is naturally included within the proposed variational method. Clearly, the evolution equations are explicitly enforced by using the parameterizations (62) of the flow rule and the hardening laws.

A careful analysis of Eq. (68) reveals the requirements necessary for consistency of the algorithm: The integrated dissipation does not depend on the pseudo stresses and furthermore,

it depends linearly on the plastic multiplier $\Delta\lambda$. This is a direct consequence of Eq. (65). More precisely,

$$\phi - g = \Sigma^{\mathrm{eq}}_{\mathrm{vol}} \neq \Sigma^{\mathrm{eq}}_{\mathrm{vol}}(\tilde{\boldsymbol{\Sigma}}, \Delta\lambda). \tag{71}$$

Hence, the difference between the yield function and the plastic potential is not affected by variables associated with dissipation. The identity (71), in turn, results from the orthogonality of the spaces $\mathcal{U}_{\Sigma_{\mathrm{vol}}} = \{\boldsymbol{\Sigma} \mid \boldsymbol{\Sigma} = a\ \mathbf{1},\ a \in \mathbb{R}\}$ and $\mathcal{U}_{\Sigma_{\mathrm{dev}}} = \{\boldsymbol{\Sigma} \mid \mathrm{tr}[\boldsymbol{\Sigma}] = 0\}$. Therefore, the additive decompositions of the Helmholtz energy, the yield function and the plastic potential are required to derive a variationally consistent method.

The proof of consistency is completed by analyzing the remaining components of the gradient of I_{inc}. Again, they yield

$$\frac{\partial I_{\mathrm{inc}}}{\partial \tilde{\boldsymbol{\Sigma}}} = \mathbf{0} \quad \overset{\Delta\lambda \neq 0}{\Rightarrow} \quad (\boldsymbol{\Sigma} - \boldsymbol{Q}_{\mathrm{k}}) : \partial^2_{\boldsymbol{\Sigma}} g = \boldsymbol{\Xi} : \partial^2_{\boldsymbol{\Xi}} g = \mathbf{0}. \tag{72}$$

Hence, Eq. (23) is again fulfilled and consequently, the plastic flow direction is compatible with the (physical) stresses and hence, it is admissible.

Remark 1. According to Section 2 (see Eq. (20)), for models fulfilling the normality rule, the stresses follow jointly from the minimization principle $\inf I_{\mathrm{inc}}$ as well. More precisely, in this case $\boldsymbol{P}$ results from the hyperelastic relation

$$\boldsymbol{P} = \frac{\partial \Psi_{\mathrm{inc}}(\boldsymbol{F}_{n+1})}{\partial \boldsymbol{F}_{n+1}} = \frac{\partial \Psi^{\mathrm{e}}(\boldsymbol{F}_{n+1})}{\partial \boldsymbol{F}_{n+1}}, \tag{73}$$

with $\Psi_{\mathrm{inc}}(\boldsymbol{F}) := \inf_{\tilde{\boldsymbol{\Sigma}}, a} I_{\mathrm{inc}}(\tilde{\boldsymbol{\Sigma}}, a, \boldsymbol{F}_{n+1})$. However, for the class of non-associative models presented in this section, the dissipation (61) depends on $\boldsymbol{\Sigma}$ and thus, it is affected by the deformation gradient. Hence,

$$\boldsymbol{P} = \frac{\partial \Psi_{\mathrm{inc}}(\boldsymbol{F}_{n+1})}{\partial \boldsymbol{F}_{n+1}} = \frac{\partial \Psi^{\mathrm{e}}(\boldsymbol{F}_{n+1})}{\partial \boldsymbol{F}_{n+1}} - \underbrace{\Delta\lambda\, \frac{\partial \Sigma^{\mathrm{eq}}_{\mathrm{vol}}}{\partial \boldsymbol{F}}}_{\neq \mathbf{0}} \tag{74}$$

with

$$\frac{\partial \Sigma^{\mathrm{eq}}_{\mathrm{vol}}}{\partial \boldsymbol{F}} = \frac{\partial \Sigma^{\mathrm{eq}}_{\mathrm{vol}}}{\partial(\mathrm{tr}[\boldsymbol{\Sigma}])} \frac{\partial(\mathrm{tr}[\boldsymbol{\Sigma}])}{\partial J}\ J\ \boldsymbol{F}^{-T}. \tag{75}$$

As a result, the size of the loading steps has to be checked carefully such that $\Delta\lambda$ (and accordingly $\Delta\lambda\ \partial\Sigma^{\mathrm{eq}}_{\mathrm{vol}}/\partial\boldsymbol{F}$) are sufficiently small. Alternatively, $\boldsymbol{P}$ can be computed in the standard manner, i.e., by utilizing $\boldsymbol{P} = \partial\Psi^{\mathrm{e}}/\partial\boldsymbol{F}$. However, it bears emphasis that the algorithm is nevertheless consistent. That is, for the limiting case $\Delta t \to 0$

$$\boldsymbol{P} = \frac{\partial \Psi_{\mathrm{inc}}(\boldsymbol{F}_{n+1})}{\partial \boldsymbol{F}_{n+1}} = \frac{\partial \Psi^{\mathrm{e}}(\boldsymbol{F}_{n+1})}{\partial \boldsymbol{F}_{n+1}} \tag{76}$$

is obtained.

4 Numerical example

The efficiency and performance of the constitutive update as advocated in the previous section are demonstrated by means of numerical analyses of a compression test (Subsection 4.1, see Fig. 1) and a shear test (Subsection 4.2). Clearly, these examples guarantee that deviatoric as

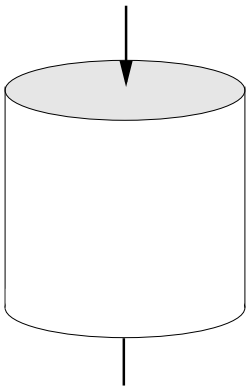

Material parameters:	von Mises	Drucker-Prager	non-associative
K [kN/m^2]	33333.3	33333.3	33333.3
μ [kN/m^2]	7143.0	7143.0	7143.0
κ [-]	0.0	0.233	0.233
Q_0^{eq} [kN/m^2]	24.24	24.24	24.24
H_{i} [kN/m^2]	50.0	50.0	50.0
H_{k} [kN/m^2]	50.0	50.0	50.0

Figure 1: Uniaxial compression test: boundary conditions and material parameters according to Eqs. (77)–(79).

well as volumetric stresses are non-vanishing and therefore, those numerical analyses represent suitable benchmarks.

For both examples, a functional of the type

$$\Psi^{\mathrm{e}} = \frac{1}{2}\,\mu\,\left(\mathrm{tr}\,[\boldsymbol{C}^{\mathrm{e}}_{\mathrm{dev}}] - 3\right) + \frac{1}{4}\,K\,\left(J^{\mathrm{e}} - 1\right)^2 \tag{77}$$

is adopted for the elastic response, while the plastic part of the Helmholtz energy is assumed to be quadratic, i.e

$$\Psi^{\mathrm{p}} = \frac{1}{2}\,H_{\mathrm{i}}\,\alpha_{\mathrm{i}}^2 + \frac{1}{2}\,H_{\mathrm{k}}\,\boldsymbol{\alpha}_{\mathrm{k}} : \boldsymbol{\alpha}_{\mathrm{k}}. \tag{78}$$

Consequently, coupled linear isotropic/kinematic hardening is considered. The model is completed by a yield function of the type

$$\phi(\boldsymbol{\Sigma}, \boldsymbol{Q}_{\mathrm{k}}, Q_{\mathrm{i}}) = ||\mathrm{dev}[\boldsymbol{\Sigma} - \boldsymbol{Q}_{\mathrm{k}}]|| + \kappa\,\mathrm{tr}[\boldsymbol{\Sigma}] - Q_{\mathrm{i}} - Q_0^{\mathrm{eq}}. \tag{79}$$

Based on Eqs. (77)–(79) three different constitutive laws have been implemented:

- Drucker-Prager model with associative evolution; Eqs. (77)–(79)
- von Mises model (Drucker-Prager model with $\kappa = 0$)
- non-associative Drucker-Prager model (Eqs. (77)–(79) and a purely deviatoric flow rule).

The material parameters used in the computations are summarized in Fig. 1. Except for the hardening parameters, they are identical to those employed in [38], if the deformations are infinitesimal small. For a physical interpretation of the variables, the interested reader is referred to [38]. For instance, $\kappa = 0.233$ corresponds to a friction angle of 30°. Obviously, since the hardening parameters are identical for all models, the mechanical response predicted by the novel constitutive update for the non-associative Drucker-Prager type model is expected to range between the limiting associative models. As a result, the correctness of the implementation can be checked easily.

4.1 Cyclic compression test

The three aforementioned constitutive models are applied to the analysis of one compression loading cycle. More precisely, loading is prescribed until a stretch of 0.9 is reached (10% shortening). Subsequently, loading is reversed. The results obtained from finite element analyses are

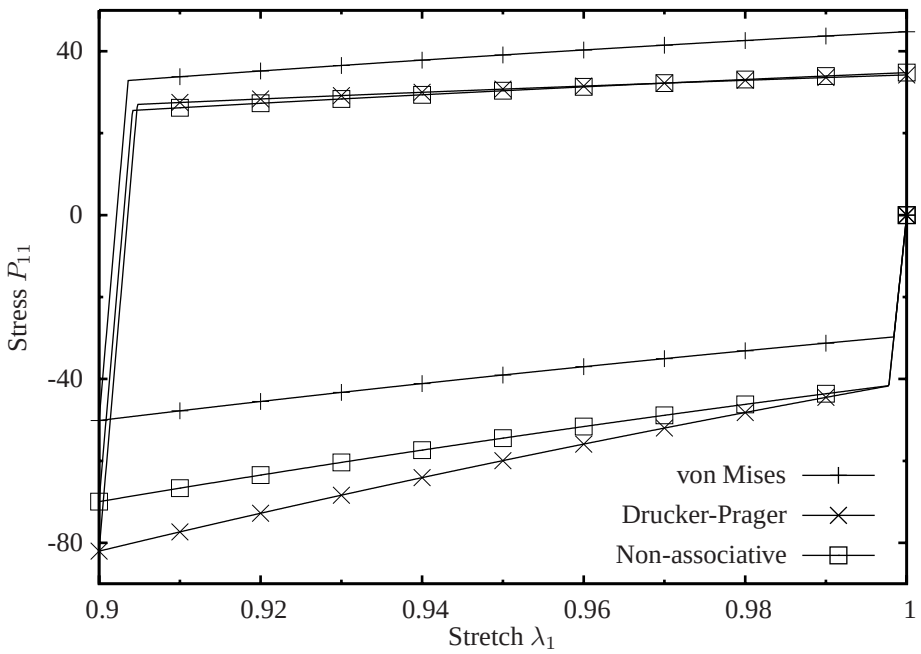

Figure 2: Uniaxial compression test: stress-strain diagrams obtained by computing one loading/unloading cycle for the three different constitutive models according to Fig. 1.

summarized in Fig. 2. As expected, the von Mises-type model predicts plastic yielding first. Furthermore, the slope of the stress-strain diagram is almost identical for the tension and the compression regime (stresses). By contrast, the Drucker-Prager model exhibits the well-known tension-compression asymmetry, i.e., the hardening effects are more dominant for compression. The non-associative version of the Drucker-Prager model as presented in the previous section features the same asymmetry – however, less pronounced. In this respect and as anticipated, the response of the non-associative constitutive law lies in the middle between both associative models.

The robustness of the discussed implementation is analyzed next, by re-computing the same problem as before. However, the size of the loading steps is now varied. As evident from Fig. 3, the results of the constitutive update do not depend on the size of the load step. Furthermore, even if relatively large loading increments are applied, the robustness of the algorithm is verified. Numerical problems did not occur.

4.2 Cyclic shear test

As a second example, a cyclic shear test is numerically analyzed. More precisely, a purely displacement-driven problem characterized by a deformation gradient of the type

$$\boldsymbol{F} = \boldsymbol{1} + (\lambda_{\mathrm{c}} - 1)\, \boldsymbol{e}_1 \otimes \boldsymbol{e}_1 + \gamma\, \boldsymbol{e}_1 \otimes \boldsymbol{e}_2 \tag{80}$$

is considered. Here and henceforth, $\boldsymbol{e}_i$ are the standard Cartesian basis vectors, $\lambda_{\mathrm{c}} \in (0, 1)$ denotes a prescribed compression stretch and γ represents the amplitude of the shear strain. Clearly, if $\lambda_{\mathrm{c}} = 1$ (vanishing compression strain), the von Mises model and the variationally consistent non-associative Drucker-Prager type extension yield almost identical results. For this reason, a non-vanishing compression strain of magnitude $\lambda_{\mathrm{c}} = 0.99$ is applied (1% compression strain). While λ_{c} is kept fixed, the shear strain γ is subsequently increased from 0 to 0.05 (5%

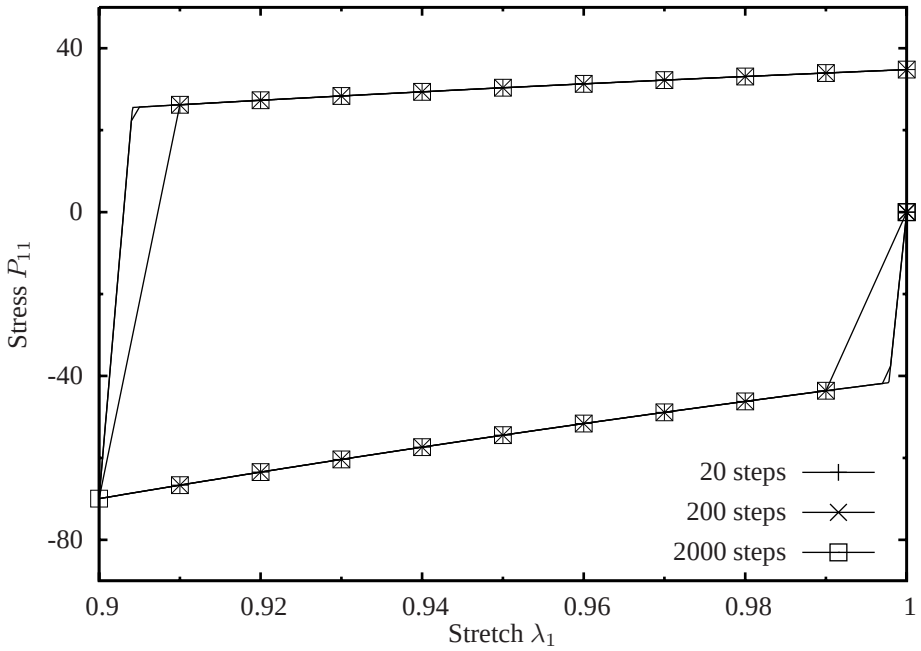

Figure 3: Uniaxial compression test: stress-strain diagrams obtained by computing one loading/unloading cycle for the non-associative constitutive model according to Fig. 1; the size of the loading steps varies between $\Delta\lambda_1 = 0.01$ (20 steps) and $\Delta\lambda_1 = 0.0001$ (2000 steps).

shear strain). The material parameters of the three different constitutive models are identically chosen as in the previous subsection (see Fig.1).

The computed results are summarized in Fig. 4. As expected and in line with the previous subsection, the non-associative model is again bounded by the two associative counterparts. Evidently, all models predict a hardening effect. However, due to the relatively small hardening moduli H_{i} and H_{k}, this effect stems mostly from the coupling between the volumetric and the deviatoric mechanical response. Consequently, the von Mises model shows the least pronounced effect. By contrast both yield functions depending on the volumetric stresses exhibit strong hardening effects.

5 Conclusion

In this paper, an enhanced *variational constitutive update* suitable for a class of non-associative plasticity theories at finite strain has been proposed. Following previously published works on variational constitutive updates, this method allows to compute the current internal variables describing plastic deformations by means of a minimization problem. Physically, one seeks to minimize the integrated stress power subjected to a constraint which is associated with the yield function. Besides this physically sound interpretation of internal states as energy minimizers, this strategy shows mathematical advantages (existence of solution) as well as numerical advantages (standard minimization problem) as well. In contrast to existing models, the advocated approach can be applied even to a broad class of non-associative evolution equations. Clearly, this represents a first important step towards a general framework for more universally valid variational constitutive update. The considered class of material models is based on a volumetric-deviatoric uncoupled response for the elastic stored energy, the yield function and the plastic potential, respectively. Prominent and frequently applied plasticity models falling

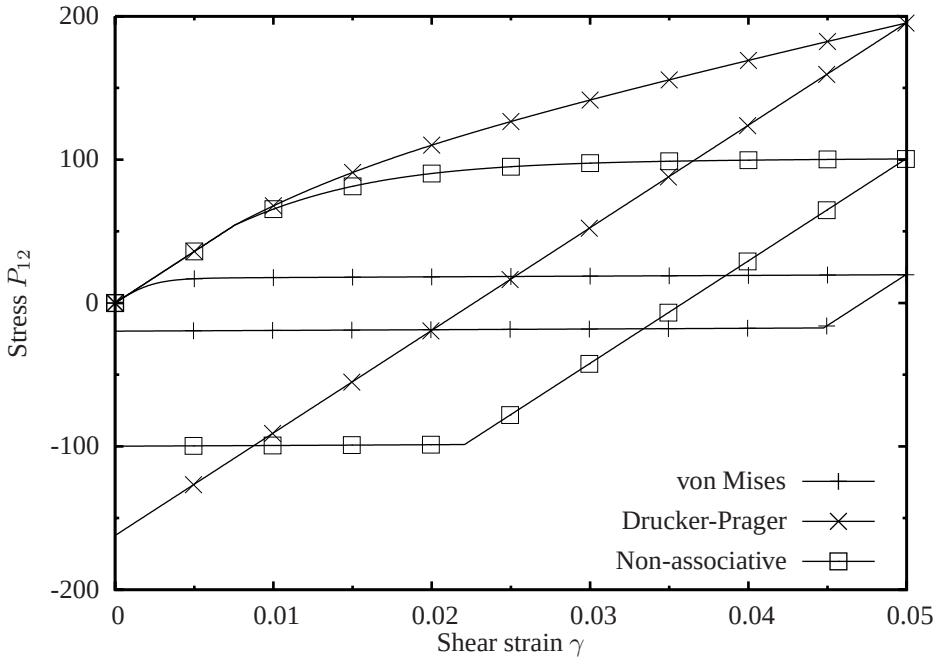

Figure 4: Cyclic shear test: stress-strain diagrams obtained by computing one loading/unloading cycle for the three different constitutive models according to Fig. 1.

into the aforementioned class are Rankine, von Mises, Hill, Drucker-Prager, Tresca, Mohr-Coulomb or crystal plasticity. The fundamental ideas required for deriving such a variationally consistent method were a convenient parameterization of the evolution equations and the hardening laws, together with an orthogonality between the spaces of purely deviatoric and purely volumetric tensors. The resulting minimization problem is formally identical to that of associative models and can be solved by employing standard gradient-type optimization schemes. The presented numerical examples demonstrated the applicability, robustness as well as the performance of the proposed implementation. By comparing the proposed variationally consistent non-associative model to its associative limiting cases, it has been found that all models show a similar efficiency, i.e., the respective CPU costs are almost identical.

References

[1] R. Hill. *The mathematical theory of plasticity*. Oxford University Press, Oxford, U.K., 1950.

[2] M. Ortiz and L. Stainier. The variational formulation of viscoplastic constitutive updates. *Computer Methods in Applied Mechanics and Engineering*, 171:419–444, 1999.

[3] R. Radovitzky and M. Ortiz. Error estimation and adaptive meshing in strongly nonlinear dynamic problems. *Computer Methods in Applied Mechanics and Engineering*, 172:203–240, 1999.

[4] C. Miehe. Strain-driven homogenization of inelastic microstructures and composites based on an incremental variational formulation. *International Journal for Numerical Methods in Engineering*, 55:1285–1322, 2002.

[5] C. Carstensen, K. Hackl, and A. Mielke. Non-convex potentials and microstructures in finite-strain plasticity. *Proc. R. Soc. Lond. A*, 458:299–317, 2002.

[6] C. Comi, A. Corigliano, and G. Maier. Extremum properties of finite-step solutions in elastoplasticity with nonlinear hardening. *International Journal for Solids and Structures*, 29:965–981, 1991.

[7] C. Comi, G. Maier, and U. Perego. Generalized variable finite element modeling and extremum theorems in stepwise holonomic elastoplasticity with internal variables. *Computer Methods in Applied Mechanics and Engineering*, 96:213–237, 1992.

[8] B. Halphen and Q.S. Nguyen. Sur les matériaux standards généralisés. *J. Mécanique*, 14:39–63, 1975.

[9] K. Hackl. Generalized standard media and variational principles in classical and finite strain elastoplasticity. *Journal of the Mechanics and Physics of Solids*, 45(5):667–688, 1997.

[10] M. Ortiz and E.A. Repetto. Nonconvex energy minimisation and dislocation in ductile single crystals. *J. Mech. Phys. Solids*, 47:397–462, 1999.

[11] J.M. Ball. Convexity conditions and existence theorems in nonlinear elasticity. *Arch. Rat. Mech. Anal.*, 63:337–403, 1978.

[12] J. Mosler and M. Ortiz. On the numerical implementation of variational arbitrary Lagrangian-Eulerian (VALE) formulations. *International Journal for Numerical Methods in Engineering*, 67:1272–1289, 2006.

[13] J. Mosler. *On the numerical modeling of localized material failure at finite strains by means of variational mesh adaption and cohesive elements*. Habilitation, Ruhr University Bochum, Germany, 2007.

[14] P. Thoutireddy and M. Ortiz. A variational r-adaption and shape-optimization method for finite-deformation elasticity. *International Journal for Numerical Methods in Engineering*, 61:1–21, 2004.

[15] J.C. Simo. Numerical analysis of classical plasticity. In P.G. Ciarlet and J.J. Lions, editors, *Handbook for numerical analysis*, volume IV. Elsevier, Amsterdam, 1998.

[16] J.C. Simo and T.J.R. Hughes. *Computational inelasticity*. Springer, New York, 1998.

[17] C. Miehe, M. Lambrecht, and J. Schotte. Computational plasticity of materials with micro-structures at finite strains based on an incremental variational formulation. In Z. Waszczyszyn and Pamin P., editors, *2. European Congress on Computational Mechanics*, Cracow, Poland, 2001.

[18] M. Ortiz and A. Pandolfi. A variational Cam-clay theory of plasticity. *Computer Methods in Applied Mechanics and Engineering*, 193:2645–2666, 2004.

[19] E. Fancello, J.-P. Ponthot, and L. Stainier. A variational formulation of constitutive models and updates in non-linear finite viscoelasticity. *International Journal for Numerical Methods in Engineering*, 65:1831–1861, 2006.

[20] L. Noels, L. Stainier, and J.-P. Ponthot. An energy momentum conserving algorithm using the variational formulation of visco-plastic updates. *International Journal for Numerical Methods in Engineering*, 65:904–942, 2006.

[21] A. Pandolfi, S. Conti, and M. Ortiz. A recursive-faulting model of distributed damage in confined brittle materials. *Journal of the Mechanics and Physics of Solids*, 54:1972–2003, 2006.

[22] Q. Yang, L. Stainier, and M. Ortiz. A variational formulation of the coupled thermo-mechanical boundary-value problem for general dissipative solids. *Journal of the Mechanics and Physics of Solids*, 33:2863–2885, 2005.

[23] Q. Yang. *Thermomechanical variational principles for dissipative materials with application to strain localization in bulk metallic glasses*. PhD thesis, California Institute of Technology, Pasadena, USA, 2004.

[24] J. Mosler and O.T. Bruhns. On the implementation of rate-independent standard dissipative solids at finite strain – variational constitutive updates. *International Journal of Plasticity*, 2008. submitted.

[25] E.H. Lee. Elastic-plastic deformation at finite strains. *Journal of Applied Mechanics*, 36:1–6, 1969.

[26] J. Lubliner. *Plasticity theory*. Maxwell Macmillan International Edition, 1997.

[27] C. Miehe. *Kanonische Modelle multiplikativer Elasto-Plastizität. Thermodynamische Formulierung und numerische Implementierung*. Habilitation, Forschungs- und Seminarbericht aus dem Bereich der Mechanik der Universität Hannover, Nr. F 93/1, 1993.

[28] J. Lubliner. On the thermodynamic foundations of non-linear solid mechanics. *International Journal of Non-Linear Mechanics*, 7:237–254, 1972.

[29] B.D. Coleman and W. Noll. The thermodynamics of elastic materials with heat conduction and viscosity. *Arch. Rational Mech. Anal.*, 13:167178, 1963.

[30] B.D. Coleman. Thermodynamics of materials with memory. *Arch. Rational Mech. Anal.*, 17:1–45, 1964.

[31] B.D. Coleman and M.E. Gurtin. Thermodynamics with internal state variables. *J. Chem. Phys*, 47:597–613, 1967.

[32] J. Mandel. *Plasticité Classique et Viscoplasticité*. Cours and Lectures au CISM No. 97. International Center for Mechanical Sciences, Springer-Verlag, New York, 1972.

[33] R.T. Rockafellar. *Convex Analysis*. Princeton University Press, 1997.

[34] C. Geiger and C. Kanzow. *Numerische Verfahren zur Lösung unrestringierter Optimierungsaufgaben*. Springer, 1999.

[35] M. Ortiz, R.A. Radovitzky, and E.A. Repetto. The computation of the exponential and logarithmic mappings and their first and second linearizations. *International Journal for Numerical Methods in Engineering*, 52(12):1431–1441, 2001.

[36] M. Itskov. Computation of the exponential and other isotropic tensor functions and their derivatives. *Computer Methods in Applied Mechanics and Engineering*, 192(35-36):3985–3999, 2003.

[37] J.C. Simo and R.L. Taylor. Quasi-incompressible finite element elasticity in principal stretches. Continuum basis and numerical algorithms. *Computer Methods in Applied Mechanics and Engineering*, 85:273–310, 1991.

[38] R.I. Borja and A.R. Regueiro. Strain localization in frictional materials exhibiting displacement jumps. *Computer Methods in Applied Mechanics and Engineering*, 190:2555–2580, 2001.